



# Dynamic finite element analysis of hip replacement edge loading: Balancing precision and run time in a challenging model

Lee Etchels<sup>a,\*</sup>, Lin Wang<sup>a,b</sup>, Jonathan Thompson<sup>a,b</sup>, Ruth Wilcox<sup>a</sup>, Alison Jones<sup>a</sup>

<sup>a</sup> Institute of Medical and Biological Engineering, School of Mechanical Engineering, University of Leeds, LS2 9JT, UK

<sup>b</sup> Deputy Synthes, St Anthony's Road, Leeds, LS11 8DT, UK

## ARTICLE INFO

### Keywords:

Total hip replacement  
Finite element analysis  
Dynamic modelling  
Mass-scaling  
Edge loading  
UHMWPE

## ABSTRACT

An important aspect in evaluating the resilience of hip replacement designs is testing their performance under adverse conditions that cause edge loading of the acetabular liner. The representation of edge loading conditions in finite element models is computationally challenging due to the changing contact locations, need for fine meshes, and dynamic nature of the system.

In this study, a combined mesh and mass-scaling sensitivity study was performed to identify an appropriate compromise between convergence and solution time of explicit finite element analysis in investigating edge loading in hip replacement devices. The optimised model was then used to conduct a sensitivity test investigating the effect of different hip simulator features (the mass of the translating fixture and mediolateral spring damping) on the plastic strain in the acetabular liner. Finally, the effect of multiple loading cycles on the progressive accumulation of plastic strain was then also examined using the optimised model.

A modelling approach was developed which provides an effective compromise between mass-scaling effects and mesh refinement for a solution time per cycle of less than 1 h. This 'Recommended Mesh' model underestimated the plastic strains by less than 10%, compared to a 'Best Estimate' model with a run time of ~190 h. Starting with this model setup would therefore significantly reduce any new model development time while also allowing the flexibility to incorporate additional complexities as required. The polyethylene liner plastic strain was found to be sensitive to the simulator mass and damping (doubling the mass or damping had a similar magnitude effect to doubling the swing phase load) and these should ideally be described in future experimental studies. The majority of the plastic strain (99%) accumulated within the first three load cycles.

## 1. Introduction

A recent development in pre-clinical testing for hip replacements requires evaluation of new designs against an international standard test (ISO14242:4), which generates contact between the femoral head and acetabular liner at both the conforming bearing surface of the liner and at the non-conforming liner rim. This test was developed to take into account incidences of hip joint subluxation after surgery, where the head and cup can separate causing loading of the liner rim region (Sato et al., 2017; Karunaseelan et al., 2021).

The ISO14242:4 tests are performed across millions of loading cycles and, particularly for hard-on-soft bearings like those using a cross-linked ultra-high-molecular-weight polyethylene (UHMWPE) liner, the relatively high loads and small contact areas can lead to a combination of

damage mechanisms including wear, plastic deformation, creep, and fatigue (Williams et al., 2003; Hua et al., 2014; Partridge et al., 2018; de Villiers and Collins, 2020). The ability to isolate these damage mechanisms would make it much easier to establish targets for device design improvement.

Computational modelling can be used to understand the relative contribution of different factors to the resulting implant damage as seen in the experimental testing, which cannot be easily done using experimental measurements. It can also allow for the investigation of additional field variables and the application of multiple alignment and load scenarios on identical geometries. There is, therefore, a need to develop a computational model that can determine the stress and strain fields within the liner with sufficient accuracy to predict deformation and damage, and that can be applied to different device designs and test

*Abbreviations:* UHMWPE, ultra-high-molecular-weight polyethylene; FE, finite element; MoP, metal-on-polyethylene; SwPL, Swing phase load.

\* Corresponding author.

E-mail address: [l.w.etchels@leeds.ac.uk](mailto:l.w.etchels@leeds.ac.uk) (L. Etchels).

<https://doi.org/10.1016/j.jmbbm.2023.105865>

Received 28 April 2022; Received in revised form 3 April 2023; Accepted 16 April 2023

Available online 17 April 2023

1751-6161/© 2023 The Authors. Published by Elsevier Ltd. This is an open access article under the CC BY license (<http://creativecommons.org/licenses/by/4.0/>).

settings. To maximise its use, this model should solve in a time-frame suitable for analyses involving multiple cycles and iterative processes such as wear (Wang et al., 2019) or fatigue modelling. Previous work has demonstrated that dynamic, inertial effects are important to include when modelling the edge loading scenario as the resulting delay of head re-location after separation substantially increases the forces experienced at the liner rim (Jahani et al., 2021). However, the inclusion of these inertial effects, alongside an elastoplastic material model and contact interactions across multiple locations were found to generate complex models with high computational cost.

Experimentally, the fixture mass and spring damping coefficient may be difficult to measure and/or control when testing occurs across multiple hip simulators, such as when comparing between different research groups or updating simulator equipment. Additionally, these values are commonly not provided in published experimental testing literature. The sensitivity of the liner contact and plastic strain results to these factors is therefore also of interest and could provide important context to experimental testing comparisons.

To facilitate practical application of such models, two competing requirements must be fulfilled. Firstly, the optimisation of the mesh, providing elements in the regions of contact which are sufficiently small to generate convergence in the local stress field. Secondly, the minimisation of the computational cost and resulting run time. The purpose of this study was to identify a modelling methodology for ISO 14242:4 testing that can minimise the run time while providing the required functionality and precision for accurate stress/strain-based device evaluation. The capability of the model was then demonstrated by investigating how plastic strain can be accumulated across multiple load cycles.

This study therefore had three aims:

1. To find the optimal modelling approach, mesh refinement, and mass-scaling settings which minimised the run time of the model and the error in the model outputs.
2. To establish the effect of the simulator specific dynamic drivers of the system, namely the fixture and component mass and the spring damping coefficient.
3. To establish the percentage of liner plastic strain accumulated over each of the first ten gait cycles.

## 2. Methods

### 2.1. Overview of approach

Prior to the work described in this study, dynamic and deformable finite element (FE) models for edge loading on hard-on-soft bearings were previously developed by Jahani et al. (2021).

The initial model settings used in the mesh density and mass-scaling (Section 2.4) optimisation were developed through a preliminary investigation. This provided the element shape, element shape function, spring setup, load profile, and symmetry boundary conditions. This preliminary work also included alternate loading scenarios to ensure wider applicability of the model. The preliminary test results are given in an open data packet (Etchels et al., 2023) and the methodological outcomes are summarised in Section 2.3.

In the current work, the modelling method was optimised with the specific aim of achieving a refined mesh that well represented the stress and strain field within the liner in a practical timeframe. To achieve this, a combination of mesh refinement and mass-scaling optimisation was investigated to find an optimal compromise. Increasing mesh refinement increased run times but provided higher accuracy, while mass-scaling decreased run times but also decreased accuracy. With multiple interacting variables affecting the model convergence and extremely long run times for unoptimised models (up to ~600 h within this study) the process to identify both converged output reference values to evaluate against, and an optimal trade-off between accuracy and run time, was

very iterative.

The optimised model, with an established error level and reduced run time, was then used to investigate the effect of experimental variation (Aim 2) and the response of the liner over multiple cycles (Aim 3).

### 2.2. Test conditions

In the ISO 14242:4 edge loading testing method, the cup and head components are positioned together and experience loading and rotations designed to simulate walking gait (ISO, 2014). The load is applied vertically, the cup is oriented relative to this to achieve the desired inclination, and the rotations are then typically applied to the head. For edge loading, an additional pre-compressed/tensioned spring is included which applies a load in the mediolateral direction. This spring force is directed to push/pull the head or cup out of alignment such that the contact location on the liner moves laterally towards the rim (Fig. 1A). When the applied loading is high, the spring is tensioned, moving the head into the cup and the contact location is on the bearing surface. When the applied load reduces, the spring causes the components to separate and the contact moves towards the rim (Fig. 1B). The location of the contact between the head and the liner is a function of the device shape and orientation, the axial load, the mediolateral spring stiffness and tension, and friction generated by the femoral head rotations.

The mesh refinement and mass-scaling study was performed using the ISO 14242:4 load case, which was the most relevant for experimental testing (Table 1).

### 2.3. Finite element model

A dynamic, deformable, explicit finite element (FE) model of a total hip replacement under ISO edge loading conditions was developed within the commercially available software package Abaqus (v2019, Dassault Systèmes, France).

For all models, the geometry used was for a 36 mm Pinnacle metal-on-polyethylene (MoP) bearing (DePuy Synthes, Leeds, UK). The outer locking features of the liner, for attachment to the shell component which was not included in this FE model, were removed to reduce the total number of elements and improve the mesh quality at the rim.

A 2.5 kg fixture mass was chosen to represent an existing test simulator (ProSim EM13, Simulation Solutions, UK). Data on experimental spring damping coefficients was not available, so a baseline value of 1 N/mm was used which would critically damp a simple 2.5 kg, 100 N/mm, mass-spring-damper system (Inman, 2001).

The bearing contact algorithm used hard penalty normal contact and penalty tangential contact with a coefficient of friction of 0.05 (Brockett et al., 2007), which was derived under concentric conditions only.

Femoral head rotations were not included in the FE model. Without these rotations, and with no anteversion applied to the cup, the edge loading test cases are symmetrical around the frontal plane. Only half of the liner was therefore modelled and the head component mass, axial load, spring stiffness, and spring damping coefficient were modified appropriately. Symmetry boundary conditions were applied to the cross-section of the liner, and it was fixed on the outer surface. The head and liner were initially positioned with no separation and as close to in contact as possible superiorly, while avoiding any overclosure of the contact surfaces.

Mass-scaling is applied to deformable elements and was therefore only required on the liner. To allow for mass-scaling, without increasing the mass of the translating component, the model was set up such that the liner remained static (fixed at the back surface) and the spring and resulting translations were applied to the analytical rigid head. As such, the mass of the actual, unscaled, loading fixture, potting cement, shell, and liner was applied to the head component and the mass-scaling was applied to the liner.

The key phases of the gait cycle, in terms of generating plastic

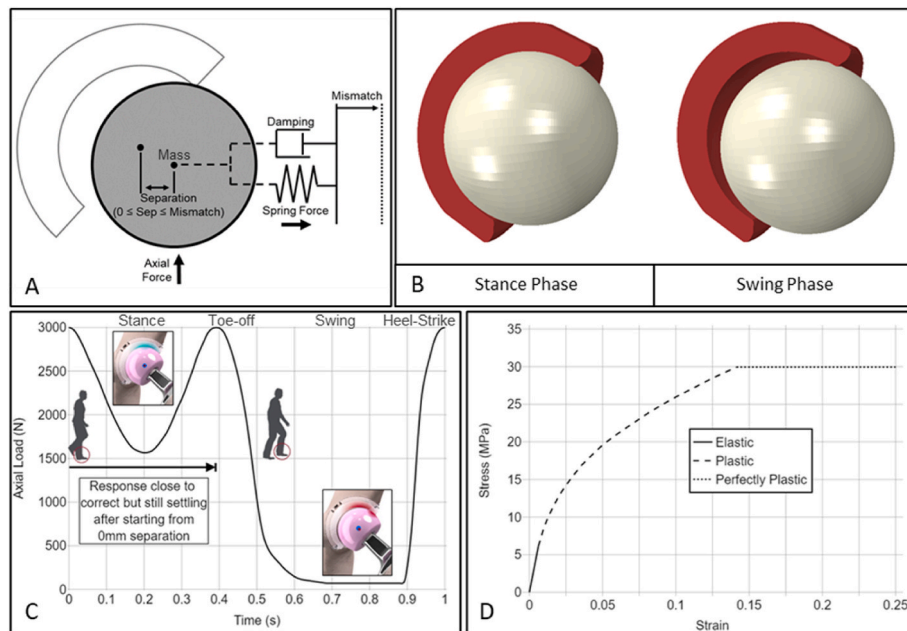


**Fig. 1.** (A) Schematic of the ISO 14242:4 mechanism for generating edge loading during swing phase. (B) View of the FE model with the head concentric at stance phase and separated at swing phase. (C) Load profile used in the analysis step of the FE model. (D) Material properties used for UHMWPE including a description of the numerical behaviour of the model after the final available data point.

**Table 1**

Description of the ISO 14242:4 load case settings and the values for the spring damping, and fixture mass which are not specified in the standard.

Inclination (°)	Spring Compression (mm)	Swing Phase Load (N)	Spring Stiffness (N/mm)	Spring Damping Coefficient (Ns/mm)	Fixture Mass (kg)
65	4	70	100	1	2.5

deformation to the liner, are swing phase where the contact is against the liner rim and heel-strike where the rapidly increasing load moves the contact from the rim towards the bearing surface. The load profile for the model was started at the first load peak during stance phase (length 1 s – Fig. 1C) from an initial 3000 N pre-load. By the second load peak, the effect of starting at a separation of 0 mm at the start of the step instead of the correct, but initially unknown, value was negligible. Results were only drawn from the second load peak through to the end of the step (~0.4 s–1 s).

Linear hexahedral C3D8R elements were used at potential contact locations on the liner rim, sweeping 50° around the rim from the frontal plane, and linear tetrahedral C3D4 elements were used for the rest of the liner geometry. Linear elements were used as they more efficiently converged for this problem (which is most likely due to the localisation of the plastic deformation (Simulia, 2019)). A swept mesh was required to produce a uniformly smooth rim geometry. This avoided imperfections that create stress risers and high local deformations and facilitated the use of hexahedral elements in this region (Fig. 2). Elements with high aspect ratio were included behind the rim as further refinement was relatively computationally expensive for the refined mesh models, and the sensitivity to this was investigated as a part of the mesh sensitivity analysis. The femoral head was modelled as an analytical rigid sphere and was therefore not discretised.

For all models an elastoplastic UHMWPE material model (Hua et al., 2014) was used for the liner (Fig. 1D). This material model included data up to a maximum stress of 29.94 MPa, after which the element behaviour was perfectly plastic. After this point elements would be able to continue to deform without any increase to the stress. This final stress

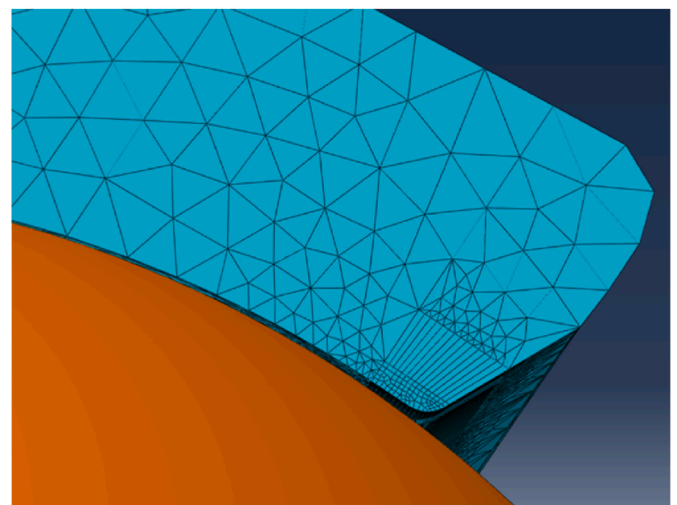


**Fig. 2.** Mesh generated on the contacted rim of the liner.

data point of 29.94 MPa represented the end of the test characterising the mechanical properties and is not indicative of the failure point of the material.

Models that could be solved with a 48 h time limit were analysed using the University of Leeds arc3 with 8 cores and up to 40 GB of RAM (Intel® Broadwell E5-2650 v4). Longer cases were analysed using a desktop pc (Intel® Xeon® E5-2643 v3, 128 GB of RAM).

To understand convergence patterns, a wide range of metrics were considered for each case. These included outputs relevant to experimental testing, outputs descriptive of the underlying damage mechanics, and outputs descriptive of the effect of mass-scaling on the mechanics and liner response and are listed in Table 2. The case descriptors given in this study refer to the settings for the associated experimental test being replicated, as opposed to the model inputs required for half-symmetry conditions. The results provided in Section 3 have been doubled where necessary to represent a full liner.

**Table 2**  
Outputs collected and compared from the finite element models.

Time Point	Output	Uses
<b>At swing phase</b>	Peak von Mises stress in the liner.	Describes the created loading environment and resulting contact conditions at the highest level of separation that contribute to the damage seen on the liner rim.
	Peak head to liner contact pressure.	
	Head to liner contact area.	
<b>Across the full cycle</b>	Lateral separation of the rotational centres of the head and liner.	Highlights moments where the loading experienced by the liner is more extreme outside of swing phase, typically due to the inclusion of inertia. Internal and kinetic energy measures show how much mass-scaling is affecting the material response of the liner to the load. Identifies how much of the liner has reached the end of the described material properties as context for how this could be affecting the other outputs.
	Peak von Mises stress in the liner.	
	Peak head to liner contact pressure.	
	Peak maximum (absolute) principal plastic strain in the liner.	
	Accumulated plastic strain in the liner (represented by plastically dissipated strain energy).	
	Peak internal (strain) and kinetic energy in the liner.	
	Original volume of all the perfectly plastically deformed elements of the liner (where the maximum stress reached 29.94 MPa).	

#### 2.4. Model optimisation

For a dynamic explicit FE analysis, smaller elements and less dense elements decrease the size of the time increment required between solutions and correspondingly increase the run time. This requirement can be countered by artificially increasing the element density, termed ‘mass-scaling’ (Li et al., 2019). This was done automatically on an element-by-element basis to achieve a target stable time increment, applying higher density increases to the smallest elements and therefore minimising the artificial increase in total mass (Simulia, 2019). This approach applied the minimum required increase in mass to achieve a particular run time. Differences in the initial geometry, meshing algorithm, or calculation of the stable time increment between software packages or investigations will alter the actual magnitude and distribution of this additional mass to some degree, however. Edge loading is a dynamic mechanism. The kinematics are therefore dependent on the total mass of the translating component, which in the case of this model was the rigid femoral head and not the mass-scaled deformable liner.

The global liner element size was varied from 2 mm to 0.25 mm. A local rim element size was varied from 1 mm to 0.01 mm. The target time increment was varied from  $1 \times 10^{-4}$  s to  $1 \times 10^{-7}$  s.

Unlike a traditional mesh sensitivity study, where precision generally increases with a more refined mesh, the addition of mass-scaling requires both parameters to be investigated together. A very fine mesh requires increased mass-scaling to maintain a practical time increment, which in turn can increase the error. As a result of these two competing sources of error it was not obvious from the outset which combination of mesh and mass-scaling would produce the best reference for a fully converged stress-strain field. After completing all cases, patterns in the model outputs were used to select a case with the most refined mesh, minimal mass-scaling error, and evidence of stress-strain convergence. This model was used as a ‘Best Estimate’ model against which the remaining, less computationally demanding, cases could be evaluated. The most suitable combination of mesh and mass-scaling was selected as a ‘Recommended Mesh’ model.

#### 2.5. Sensitivity to simulator-dependent parameters

From the ‘Recommended Mesh’ model described in Section 2.4, the fixture mass was varied independently from 0.5 kg to 5 kg in 0.5 kg increments (resulting in theoretical mass-spring-damper damping ratios of 2.2 to 0.7). The spring damping coefficient was independently varied

from 0 N/mm to 2 N/mm in increments of 0.25 N/mm (resulting in theoretical mass-spring-damper damping ratios of 0–2). The mass was then varied as before but with a corresponding change in the damping coefficient to result in a theoretical damping ratio of 1 (critically damped) for each case. To provide context for the size of the changes caused by the mass and damping compared to a common experimental input parameter, models were also analysed with the baseline 2.5 kg and 1 N/mm settings and swing phase loads of 150 N–300 N in 50 N increments. These case descriptions are also tabulated in the associated data packet.

Additionally, to investigate the effect of excluding momentum through static modelling of this problem while maintaining compatibility between models, a case was analysed using the ‘Recommended Mesh’ model but where the load profile was scaled through time by a factor of 10, resulting in one 10 s long cycle with a reduced loading rate.

#### 2.6. Plastic strain across multiple cycles

With the ‘Recommended Mesh’ model, and the ISO load case, the accumulation of plastic strain as predicted by the FE model was investigated at each time point across multiple load cycles to understand the key instances and drivers for the creation of damage due to edge loading. Ten 1 Hz load cycles were analysed as this provided enough time for the cycle-to-cycle variations to become negligible.

### 3. Results

#### 3.1. Model optimisation

The ‘Best Estimate Model’ was found to be the one that had a 0.25 mm global element size, 0.025 mm rim element size, and target time increment of  $1 \times 10^{-6}$  s. This model had a run time of ~190 h and was therefore not suitable for running parametric tests with many cases. Models with a finer mesh, down to 0.01 mm, were not used as a ‘Best Estimate’ due to errors introduced by the increased effect of mass-scaling which, due to the excessive run times, could not be compensated for with a smaller target time increment.

With mass-scaling applied to allow for a time increment of  $1 \times 10^{-5}$  s, mesh densities with a run time <30 min predicted lower peak and total plastic strain than the Best Estimate Model (Fig. 3A). The ‘Recommended Mesh Model’ was found to have a 1 mm global element size, 0.075 mm rim element size, and target time increment of  $1 \times 10^{-5}$  s. It had a run time of ~40 min (Fig. 3A) and provided the best balance of run-time to convergence. This model underestimated the peak and total plastic strain by 7% and 9%, respectively, compared to the Best Estimate Model and refining the high aspect ratio elements behind the rim to use 4x the number of elements in that region altered the peak plastic strain by less than 5%. The largest convergence errors for this model for all of the outputs described in Table 2 were a 25% overestimation of the swing phase contact area and a 15% underestimation of the volume of perfectly plastic liner elements compared to the Best Estimate Model.

For the ‘Recommended Mesh Model’, with a run time of 0.66 h, changing the target time increments to  $1 \times 10^{-4}$  s, and  $1 \times 10^{-6}$  s resulted in run times of 0.15 h, and 5.66 h, respectively. Excessive mass-scaling had the greatest effect on the total plastic strain, volume of perfectly plastic elements, and peak liner internal and kinetic energies. Mass-scaling to achieve a time increment of  $1 \times 10^{-5}$  s had negligible effect on the results and reduced run times by a factor of ~9 when compared to the  $1 \times 10^{-6}$  s time increment. Increasing the mass-scaling to  $1 \times 10^{-4}$  s resulted in clear mass-scaling errors in the response (Fig. 3B). Mass-scaling to achieve a  $1 \times 10^{-5}$  s stable time increment increased the mass of the liner by approximately 1000x, however this was not uniformly distributed. The maximum change in mass of any element was ~2000x.

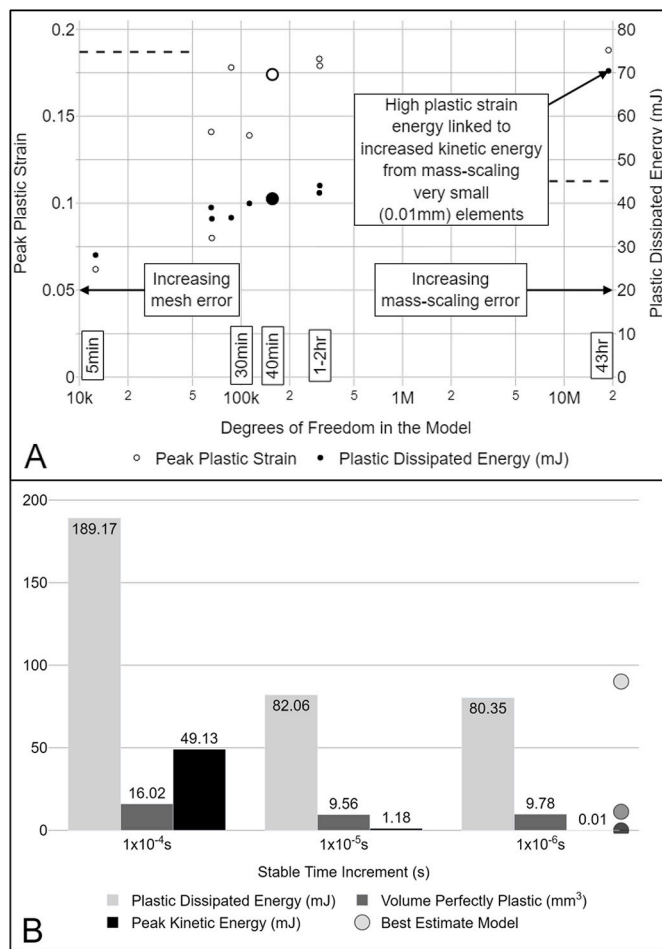


**Fig. 3.** (A) Mesh sensitivity test for the effect of element size on the peak absolute principal plastic strain and total dissipated plastic strain energy in the liner at the end of the test. Mass-scaling used with a target stable time increment of  $1 \times 10^{-5}$  s. Larger marker points indicate results from the final, recommended, model from this study. Approximate model run times are given along the x axis for reference. Values from the ‘Best Estimate Model’ are shown as broken horizontal lines from each vertical axis. (B) Effect of three different levels of mass-scaling (described by the target time increment) on the total dissipated plastic strain energy, sum of the original volume of all elements that reached the perfectly plastic region of the material definition used in this study at any point in the settled loading, and peak kinetic energy of the liner material for the ‘Recommended Mesh Model’ in (A). Values from the ‘Best Estimate Model’ are shown by markers to the right.

### 3.2. Sensitivity test

Using the ‘Recommended Mesh Model’, the maximum separation values were relatively insensitive to changes in the mass, damping coefficient, or both. The largest change from the baseline case (2.5 kg fixture mass, 1 N/mm damping coefficient) was 0.3%. Clear trends were shown linking stresses, contact areas, and contact pressures to changes in the mass, damping, or both, however the effect sizes were generally small (<10%). There was a larger effect on the peak (Fig. 4A) and total (Fig. 4B) plastic strain values (largest changes from the ‘Recommended Mesh Model’, across all cases, were -14% and 47% respectively). The largest relative changes (up to 200%) were seen in the original volume of the elements in the model that exceeded the maximum stress of the included material model (29.94 MPa), and had therefore become perfectly plastic. For context, the maximum original volume of elements that had reached 29.94 MPa across all cases was 28 mm<sup>3</sup> (~0.2% of the total liner), and the original volume of the elements that had plastically deformed for the ‘Best Estimate Model’ was around 1800 mm<sup>3</sup> (10% of

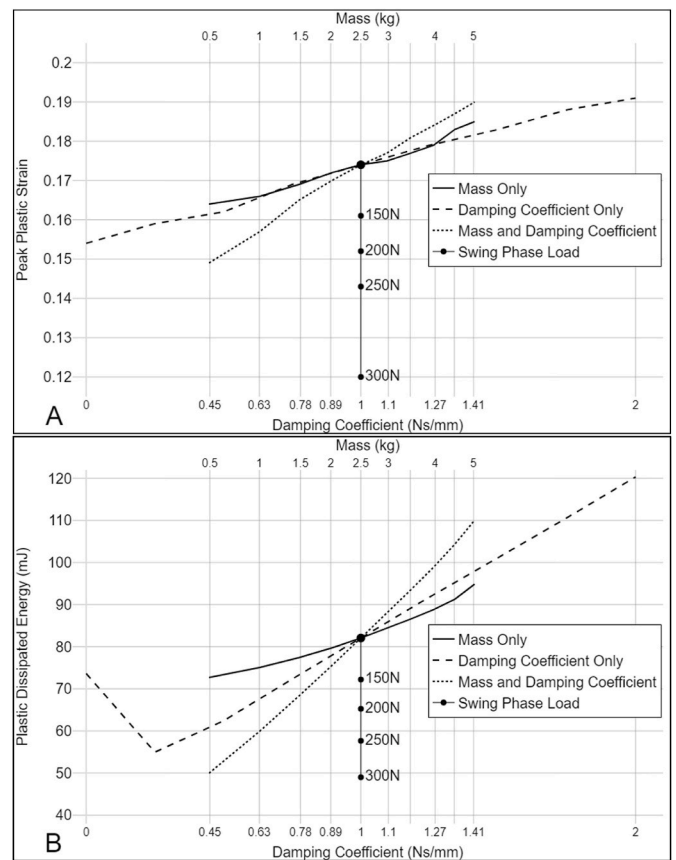


**Fig. 4.** Sensitivity of (A) the peak absolute principal plastic strain, and (B) the plastically dissipated strain energy to variations in the mass (with constant damping), damping (with constant mass), and a range of combined mass and damping coefficient combinations that all result in a theoretically critically damped mass-spring-damper system. Model used was the ‘Recommended Mesh Model’. For context, the changes in plastic strain and energy for a series of different swing phase loads, using the baseline 2.5 kg 1 N/mm settings, are included as a sensitivity comparison to an input variable from the test.

the total liner). The sensitivity of the peak plastic strain to the range of simulator dynamics inputs considered was similar in magnitude to changing the load case from a 70 N swing phase load to a ~150 N–200 N swing phase load. For the total plastic strain, it was similar to changing to a ~150 N–300 N swing phase load.

The acceleration of the head when moving onto the rim at toe-off and away from the rim at heel-strike was higher when the fixture mass was reduced. Slower acceleration of the head at heel-strike would increase the time required for the head to move off the rim. As the load increases with time, independent of the contact location, this would allow the axial load to increase to a higher value before the contact moved to the bearing surface (Etchels et al., 2019).

Increasing the length of the load cycle from 1 s to 10 s, to reduce the effects of inertia, caused a reduction in the peak absolute principal plastic strain of 20% to 0.14, and a reduction in the dissipated plastic strain energy of 60% to 34 mJ.

### 3.3. Plastic strain across multiple cycles

Using the Recommended Mesh Model, with mass-scaling to a  $1 \times 10^{-5}$  s time increment, plastic strain continued to accumulate over several cycles (Fig. 5). The majority (87%) of the final plastic dissipated strain energy after 10 cycles developed in the first load cycle, up to 96% at the end of the second load cycle, and 99% at the end of the third load cycle. This deformation predominantly occurred at heel-strike as the

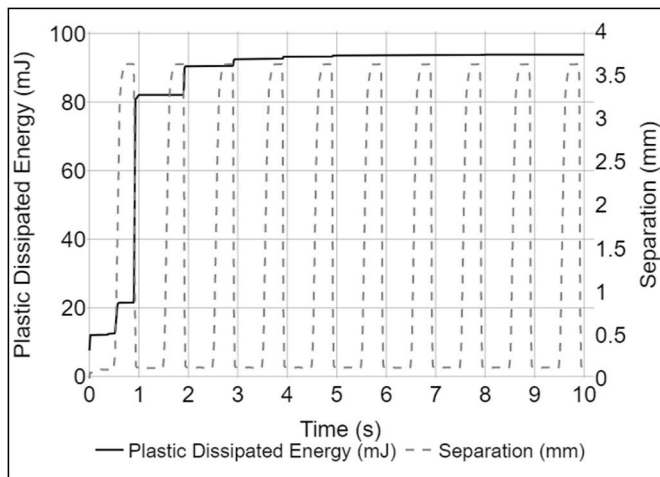


Fig. 5. Separation and plastically dissipated strain energy through time across 10 1 Hz load cycles.

separation sharply reduced.

#### 4. Discussion

The results of this study showed plastic deformation at the rim of a liner up to a maximum principal (absolute) plastic strain of  $\sim 0.2$ . Hua et al. (2014) reported maximum equivalent plastic strains of  $\sim 0.07$  using a static modelling approach (with  $65^\circ$  cup inclination, 2 mm fixed separation and a 2500 N load). Although the load cases are not directly comparable, the trend towards lower plastic strain in conditions with lower inertia were reflected in the current work, where increasing the length of the load cycle showed a reduction in plastic strain of the liner. Jahani (2017) reported maximum equivalent plastic strains of  $\sim 0.09$  at  $65^\circ$  cup inclination, 4 mm mismatch, and a 70 N swing phase load using a dynamic model with a coarser mesh density on the rim. Capturing the peak strain values for the prediction and ranking of failure risks between designs and materials therefore appears to require dynamic modelling and a refined mesh as described in this study.

The combination of a dynamic system, with contact moving across multiple portions of the surface, and a relatively long time period for the analysis creates a computationally challenging scenario. The use of symmetry conditions when appropriate, application of the translations at a rigid head instead of the liner, and the load step pattern described in this study allow for the minimisation of the run time and therefore increased mesh refinement. For any edge loading investigation of a hard-on-soft bearing, the ideal compromise between mesh refinement and amount of mass-scaling will differ based on the outputs of interest, load cases, and geometry and material of the design. The results presented here, and additional cases provided in the associated dataset, will provide both a suitable starting point and context on how to optimise the model and drastically speed up model development.

##### 4.1. Considerations for future computational studies

The work here highlights a number of considerations for future computational studies, and areas where limitations in the available data may have an effect.

First, the peak liner stresses reached the limit of the generic UHMWPE material properties used in this study, allowing additional stress-free deformation in these liner elements. This material model represents only a small part of the deformation range of these polymers. Malito et al. (2018) compared multiple, clinically relevant, forms of UHMWPE and reported mean true ultimate tensile strength values ranging from 152 MPa to 229 MPa. Material properties for UHMWPE are often given and used to a true strain of  $\sim 0.12$  (Malito et al., 2018).

Beyond true strains of 0.14, the material model used in this study was perfectly plastic and did not provide mechanical support, and as such the values above this should be considered only as indicators of the need for more extensive properties and of general trends in the response. With a material model representative of UHMWPE behaviour up to its true ultimate tensile strength, there would likely be less plastic deformation as the elements exceeding yield continued to provide resistance. Furthermore, when considering multiple load cycles, viscoelastic and viscoplastic properties are likely to become important (Rohrl et al., 2005; Penmetsa et al., 2006; Glyn-Jones et al., 2008; Zeman et al., 2018), although the time frame over which they would become significant is unknown.

Second, the mesh used in this study included long, thin, elements behind the refinement of the rim (Fig. 2). For the cases considered, the effect on the results was seen to be small, however this would not be recommended for more general or wide-ranging studies where the stress state in this region might play a larger role in the response.

Third, dynamic implicit modelling was considered for this work. However dynamic explicit modelling is recommended for very non-linear problems where solver convergence with implicit methods can be difficult and slow. Even with a dynamic implicit model a relatively large number of increments would still be required to capture and output damage at all important points in the cycle.

Finally, one of the justifications for selecting a damping coefficient for a critically damped system, when the experimental values are uncertain, is to maximise the stability of the model solution. This work has shown that stable solutions can be reached without any damping at the spring when appropriate modelling techniques are applied.

##### 4.2. Considerations for experimental work

The results from this study have implications for simulator studies under ISO 14242:4. The sensitivity to fixture mass and spring damping has been compared to the sensitivity to different swing phase loads. This can be used to aid in planning and interpreting device testing. The maximum separations were relatively insensitive to fixture mass and spring damping coefficient as surrogates for simulator design differences. Therefore, maximum separation results from different simulators, and different models of simulator, with the same inputs should be relatively consistent.

The fixture mass and spring damping coefficient also had limited effect on the peak and swing phase contact pressures, which may indicate that large differences in wear between different simulators following the same inputs would not be expected unless related to the fatigue/damage state of the material.

There will be a relatively large difference in the impetus of an underdamped and overdamped system at toe-off and heel-strike when the components move relative to each other. Given that there is little change in maximum separation but increases in peak and total plastic strain and the volume of elements in the perfectly plastic region of the material properties, the liner appeared to absorb any additional energy as localised plastic deformation. Differences in simulator setup may therefore drive differing liner damage results under the same input conditions, and publication of the translating fixture and component mass and spring damping coefficients may help understand these differences.

By analysing multiple load cycles, it was also shown that plastic deformation continues to accumulate beyond the first cycle, and that when not considering fatigue or creep properties this damage settles in less than five load cycles. After five load cycles, the rim had compressed by 0.14 mm, with the plastic strain concentrated a further 0.1 mm below the surface. Given that these plastic strains were generated in the first few cycles, it would be possible to further interpret experimental simulator data where there is accurate measurement of rim wear (Partridge et al., 2018), by considering whether or not the wear had reached this subsurface plastic region.

#### 4.3. *In vivo* conditions

The ISO 14242:4 test does not focus on recreating physiological instability motion patterns or rim loading forces. This is due to a combination of the spread and uncertainty in the *in vivo* values, and the practical limitations of existing test capabilities in terms of the loads and motions that can be achieved. Verified and validated computational models (ASME, 2018) could bridge the gaps between the idealised testing methodology and *in vivo* conditions through greater flexibility in loading and constraints, and much reduced development time and cost for test variations.

For some patients contact between the femoral head and liner rim could occur frequently. This could be due to the activities they perform (Blumenfeld et al., 2011), the ways in which they perform those activities (Lombardi Jr. et al., 2000), the specific implant choice and position (Dennis et al., 2001; Komistek et al., 2002), or surrounding bone and tissue morphology and health (Ha et al., 2007; Glaser et al., 2008; DeCook et al., 2020). The idealised testing attempts to ensure that the specific combinations of device geometries and materials being proposed are no less capable at performing under rim loading than predicate devices. Experimental testing in general (and industry standard testing in particular) is focused on generating repeatable and consistent methods for comparing devices. It is not necessarily well suited to investigating the wide range of motions and mechanisms, with all the associated variability of patients and treatment options, that could occur *in vivo*. Although there is currently no experimental plastic strain data known to the authors against which the damage predictions of this model could be validated, previous work has compared against experimental simulator kinematics (Jahani, 2017; Etchels et al., 2019). The developed methodology herein, however, can be used to integrate modelling with future experimental studies and the ongoing characterisation of crosslinked UHMWPE failure properties (Sirimamilla, Furmanski and Rinnac, 2013; Patten et al., 2014; Ansari et al., 2016). It is anticipated that an approach can then be validated that would support the use of computational modelling to investigate a much wider range of clinical scenarios.

#### 5. Conclusions

Finite element models to support ISO 14242:4 testing can be developed to run in <1 h while capturing both the important dynamic aspects of the kinematics and generating accurate stress-strain results. Identifying the necessary combination of mesh refinement and mass-scaling to achieve this can be extremely time consuming and therefore a suitable starting point, which will drastically reduce development time, has been provided in this study. For the given combination of geometry, material properties, and the ISO loading scenario the mass of an experimental fixture and the damping coefficient of the separation-inducing spring were both shown to affect the accumulation of plastic strain in the liner which may explain some differences between experimental simulators. The liner plastic strain was also shown to increase over the first ~5 loading cycles, which can be captured computationally now when required due to the now decreased run times. Plastic strains recorded with the combination of dynamic modelling and mesh refinement were higher than previously published and this highlights a need for extended characterisation of these clinical UHMWPE materials. As always, it is important to reiterate that the suitability of the recommendations provided in this study will need to be confirmed in line with modelling best practice, supported by the provided sensitivity testing.

#### CRediT authorship contribution statement

**Lee Etchels:** Writing – original draft, Visualization, Validation, Software, Methodology, Investigation, Formal analysis, Data curation, Conceptualization. **Lin Wang:** Writing – review & editing, Resources, Methodology, Funding acquisition. **Jonathan Thompson:** Writing –

review & editing, Supervision, Funding acquisition. **Ruth Wilcox:** Writing – review & editing, Supervision, Funding acquisition. **Alison Jones:** Writing – review & editing, Supervision, Funding acquisition.

#### Declaration of competing interest

The authors declare the following financial interests/personal relationships which may be considered as potential competing interests: Authors are in receipt of research funding from the UK Engineering and Physical Sciences Research Council (EPSRC) (RW, AJ, LE), DePuy Synthes (AJ, RW) and Versus Arthritis (RW). LW and JT are full-time employees of DePuy Synthes.

#### Data availability

Data is included in a repository and referenced in the paper.

#### Acknowledgements

This work was supported by the UK Engineering and Physical Sciences Research Council [EPSRC - grant EP/N02480X/1]; components and CAD files were supplied by DePuy Synthes. The EPSRC had no involvement with the study design. DePuy Synthes provided input through the affiliated co-authors. This work was undertaken on ARCC3, part of the High Performance Computing facilities at the University of Leeds, UK.

#### References

- Ansari, F., et al., 2016. Notch fatigue of ultrahigh molecular weight polyethylene (UHMWPE) used in total joint replacements. *J. Mech. Behav. Biomed. Mater.* 60, 267–279. <https://doi.org/10.1016/j.jmbbm.2016.02.014>. Elsevier.
- ASME, 2018. V V 40 - 2018 Assessing Credibility of Computational Modeling through Verification and Validation: Application to Medical Devices.
- Blumenfeld, T.J., et al., 2011. *In vivo* assessment of total hip femoral head separation from the acetabular cup during 4 common daily activities. *Orthopedics* 34 (6). <https://doi.org/10.3928/01477447-20110427-06>.
- Brockett, C., et al., 2007. Friction of total hip replacements with different bearings and loading conditions. *J. Biomed. Mater. Res. B Appl. Biomater.* 81 (2), 508–515. <https://doi.org/10.1002/jbm.b.30691>.
- DeCook, C.A., et al., 2020. *In vivo* determination and comparison of total hip arthroplasty kinematics for normal, preoperative degenerative, and postoperative implanted hips. *J. Arthroplasty* 35 (2), 588–596. <https://doi.org/10.1016/j.arth.2019.08.057>. Elsevier Ltd.
- Dennis, D.A., et al., 2001. *In vivo* determination of hip joint separation and the forces generated due to impact loading conditions. *J. Biomech.* 34 (5), 623–629.
- Etchels, L., et al., 2019. Computationally efficient modelling of hip replacement separation due to small mismatches in component centres of rotation. *J. Biomech.* 95. <https://doi.org/10.1016/j.jbiomech.2019.07.040>. The Author(s).
- Etchels, L.W., et al., 2023. Dataset Supporting the Publication Dynamic Finite Element Analysis of Hip Replacement Edge Loading: Balancing Precision and Run Time in a Challenging Model. <https://doi.org/10.5518/1157>.
- Glaser, D., et al., 2008. *In vivo* comparison of hip mechanics for minimally invasive versus traditional total hip arthroplasty. *Clin. Biomech.* 23 (2), 127–134. <https://doi.org/10.1016/j.clinbiomech.2007.09.015>.
- Glyn-Jones, S., et al., 2008. The creep and wear of highly cross-linked polyethylene: a three-year randomised, controlled trial using radiostereometric analysis. *J. Bone Joint Surg. - Series B* 90 (5), 556–561. <https://doi.org/10.1302/0301-620X.90B5.20545>.
- Ha, Y.C., et al., 2007. Ceramic liner fracture after cementless alumina-on-alumina total hip arthroplasty. *Clin. Orthop. Relat. Res.* 458, 106–110. <https://doi.org/10.1097/BLO.0b013e3180303e87>.
- Hua, X., et al., 2014. Contact mechanics of modular metal-on-polyethylene total hip replacement under adverse edge loading conditions. *J. Biomech.* 47 (13), 3303–3309. <https://doi.org/10.1016/j.jbiomech.2014.08.015>.
- Inman, D., 2001. Critical damping. In: Braun, S. (Ed.), *Encyclopedia of Vibration*. Elsevier, pp. 314–319.
- ISO, 2014. 'ISO 14242-1: Implants for Surgery - Wear of Total Hip-Joint Prostheses', Part 1: Loading And Displacement Parameters for Wear-Testing Machines and Corresponding Environmental Conditions for Test.
- Jahani, F., 2017. Modelling of Dynamic Edge Loading in Total Hip Replacements with Ceramic on Polyethylene Bearings, Mechanical Engineering. University of Leeds.
- Jahani, F., et al., 2021. Importance of dynamics in the finite element prediction of plastic damage of polyethylene acetabular liners under edge loading conditions. *Med. Eng. Phys.* 95 (August), 97–103. <https://doi.org/10.1016/j.medengphy.2021.07.010>. Elsevier Ltd.

- Karunaseelan, K.J., et al., 2021. Capsular ligaments provide a passive stabilizing force to protect the hip against edge loading. *Bone and Joint Res.* 10 (9), 594–601. <https://doi.org/10.1302/2046-3758.109.BJR-2020-0536.R1>.
- Komistek, R.D., et al., 2002. In vivo comparison of hip separation after metal-on-metal or metal-on-polyethylene total hip arthroplasty. *J Bone Joint Surg Am* 84-A (10), 1836–1841.
- Li, L., et al., 2019. Effects of mass scaling on finite element simulation of the cold roll-beating forming process. *IOP Conf. Ser. Mater. Sci. Eng.* 490 (5) <https://doi.org/10.1088/1757-899X/490/5/052019>.
- Lombardi Jr., A.V., et al., 2000. An in vivo determination of total hip arthroplasty pistoning during activity. *J. Arthroplasty* 15 (6), 702–709. <https://doi.org/10.1054/arth.2000.6637>, 2000/10/06.
- Malito, L.G., et al., 2018. Material properties of ultra-high molecular weight polyethylene: comparison of tension, compression, nanomechanics and microstructure across clinical formulations. *J. Mech. Behav. Biomed. Mater.* 83 (March), 9–19. <https://doi.org/10.1016/j.jmbbm.2018.03.029>.
- Partridge, S., et al., 2018. A novel method to measure rim deformation in UHMWPE acetabular liners. *Med. Eng. Phys.* 59, 56–62. <https://doi.org/10.1016/j.medengphy.2018.04.023>.
- Patten, E.W., et al., 2014. Quantifying cross-shear under translation, rolling, and rotation, and its effect on UHMWPE wear'. *Wear*. Elsevier 313 (1–2), 125–134. <https://doi.org/10.1016/j.wear.2014.03.001>.
- Penmetsa, J.R., et al., 2006. Influence of polyethylene creep behavior on wear in total hip arthroplasty. *J. Orthop. Res.* 24 (March), 422–427.
- Rohrl, S., et al., 2005. In vivo wear and migration of highly cross-linked polyethylene cups a radiostereometry analysis study. *J. Arthroplasty* 20 (4), 409–413. <https://doi.org/10.1016/j.arth.2004.09.040>.
- Sato, T., et al., 2017. Dynamic femoral head translations in dysplastic hips. *Elsevier Clin. BioMech.* 46, 40–45. <https://doi.org/10.1016/j.clinbiomech.2017.05.003>. February 2013.
- Simulia, 2019. *Abaqus 6.19 Documentation*.
- Sirimamilla, P.A., Furmanski, J., Rimnac, C.M., 2013. Application of viscoelastic fracture model and non-uniform crack initiation at clinically relevant notches in crosslinked UHMWPE. *J. Mech. Behav. Biomed. Mater.* 17, 11–21. <https://doi.org/10.1016/j.jmbbm.2012.07.008>. Elsevier.
- de Villiers, D., Collins, S., 2020. Wear of large diameter ceramic-on-ceramic hip bearings under standard and microseparation conditions', *Biotribology*. Elsevier 21 (January), 100117. <https://doi.org/10.1016/j.biotri.2020.100117>.
- Wang, L., et al., 2019. Finite element analysis of polyethylene wear in total hip replacement : a literature review. *Proc. Inst. Mech. Eng. H*. <https://doi.org/10.1177/0954411919872630>.
- Williams, S., et al., 2003. Wear and deformation of ceramic-on-polyethylene total hip replacements with joint laxity and swing phase microseparation. *Proc. Inst. Mech. Eng. H* 217, 147–153.
- Zeman, J., et al., 2018. UHMWPE acetabular cup creep deformation during the run-in phase of THA's life cycle. *J. Mech. Behav. Biomed. Mater.* 87, 30–39. <https://doi.org/10.1016/j.jmbbm.2018.07.015>, 2018/07/22.